All Inorganic Semiconductor Nanowire Mesh for Solar Water Splitting

Bin Liu[1,4], Cheng Hao Wu[1,3], Jian Wei Miao[4], Peidong Yang[1,2,3,★]

[1]Department of Chemistry, University of California, Berkeley, California 94720, USA

[2]Department of Materials Science and Engineering, University of California, Berkeley, California 94720, USA

[3]Materials Sciences Division, Lawrence Berkeley National Laboratory, Berkeley, California 94720, USA

[4]School of Chemical and Biomedical Engineering, Nanyang Technological University, Singapore 637459, Singapore

★e-mail: p_yang@berkeley.edu

The generation of chemical fuels via the direct solar-to-fuel conversion from a fully integrated artificial photosynthetic system is an attractive approach to supply clean energy, but so far there has yet to be a system that even comes close to the acceptable efficiency and durability and can be manufactured at a reasonable cost. Here, we show that a semiconductor mesh made from all inorganic nanowires can achieve self-driving overall water-splitting without using any electron mediators. Free-standing nanowire mesh networks could be made in large scales using solution synthesis and vacuum filtration, making this idea attractive for low cost commercial implementation.

Photoelectrolysis of water using semiconductors both as the light absorbing material and energy converter, which mimics the natural photosynthesis, is one of the most interesting ways to achieve clean and renewable energy systems. Two photocatalyst systems for overall solar water-splitting, including a single-photon system and a two-photon system have been studied extensively.[1-10] Unfortunately, most of the photocatalysts in a single-photon system, which can satisfy both the energy and band edge requirements, are wide bandgap semiconductor oxides.[6,11] The intrinsic materials limitations associated with wide bandgap semiconductors limit photon absorption only to the ultraviolet portion of the solar spectrum. Development of photocatalysts with visible light response has been sought for efficient utilization of solar energy. It has been shown that GaP,[12,13] Fe_2O_3,[14,15] WO_3,[16] $BiVO_4$,[17,18] TaON,[19] Ta_3N_5,[20] Rh-$SrTiO_3$,[21,22] and

LaTiO$_2$N[23] have visible activities for solar water-splitting; however, none of them can achieve hydrogen and oxygen evolution simultaneously. In the 1970s, Nozik proposed an appealing idea of photochemical diodes for overall water-splitting.[24] The merit of the photochemical diode is to couple together a photocathode and a photoanode made of small bandgap semiconductors (which by themselves cannot achieve overall water-splitting) and utilize the combined photovoltages to drive the spontaneous solar water-splitting, so that a larger part of the solar spectrum can be absorbed to achieve higher energy conversion efficiency. Later on, this idea was extended to semiconductor particulate photocatalyst system based on the z-scheme.[8,9,19,22,25] The z-scheme is composed of a hydrogen-evolving photocatalyst, an oxygen-evolving photocatalyst and an electron mediator for shuttling the photogenerated carriers between the hydrogen- and oxygen-evolving photocatalysts. However, the frequently used ionic electron mediators such as Fe^{2+}/Fe^{3+} and I^-/IO_3^- in z-scheme not only restricts the materials choices for photocatalysts, but also may cause negative effects such as back reactions and undesirable light shielding.[25]

To develop an efficient artificial photosynthetic system, it is necessary: (1) to develop semiconductor materials which absorb in the visible region of solar spectrum, (2) to design architectures for effective capture and conversion of sunlight, at the same time, allowing easy transport of protons and gas products, (3) to develop robust ion-conducting membranes which are impermeable to the gas products, and (4) to integrate each individual component into a complete and functioning system.[26]

In the present study, we developed a new architecture for spontaneous overall water-splitting. In this architecture, semiconductor photocatalysts were synthesized as one-dimensional nanowires, which were assembled into free standing, paper-like mesh films for solar water-splitting. The large aspect ratio of semiconductor nanowires allows for the formation of intertwined and porous nanowire networks. The porous structure of nanowire mesh networks can benefit photochemical reactions by decoupling directions for light absorption and charge carrier extraction as well as providing a large area of catalytic surfaces. Furthermore, the porous structure can also facilitate proton transport and gas evolution. In our proof-of-concept, we developed a two-photon system based on BiVO$_4$ and Rh-SrTiO$_3$ nanowires for overall water-splitting, where BiVO$_4$ nanowires act as a photoanode for water oxidation and Rh-SrTiO$_3$ nanowires work as a photocathode for water reduction.

To test the combination of materials for overall solar water-splitting, we first made two photoelectrodes of $BiVO_4$ and $Rh-SrTiO_3$ using sol-gel method followed by spin-coating on fluorine-doped SnO_2 (FTO) substrates (Supplementary Methods). After loading the co-catalyst (CoO for $BiVO_4$ and Ru for $Rh-SrTiO_3$) on the surface of photoelectrodes, a photoelectrochemical cell consisting of a $Rh-SrTiO_3$ photocathode and a $BiVO_4$ photoanode was constructed. Photoelectrochemical water-splitting was carried out under visible light ($\lambda \geq 400$ nm) in a sealed reactor without applying any external bias. Steady photocurrent was obtained, which agrees well with the evolution rate of hydrogen (Fig. 1). The amount of hydrogen evolved was nearly twice as much as that of evolved oxygen and close to half amount of electrons which had passed through the external circuit, indicating the occurrence of self-driving photoelectrolysis of water. Thus, the combination of $BiVO_4$ and $Rh-SrTiO_3$ can lead to spontaneous splitting of water to generate hydrogen and oxygen under visible light irradiation.

$SrTiO_3$ is a perovskite material with a cubic crystal structure. The necessity of breaking crystal symmetry makes direct synthesis of anisotropic $Rh-SrTiO_3$ nanowires difficult. In this study, we adopted a general self-templated ion exchange method for preparing $Rh-SrTiO_3$ and $BiVO_4$ nanowires in large scales for assembling nanowire mesh films. The self-templated method involves two steps: growth of nanowire templates ($H_2Ti_3O_7$ nanowires for $Rh-SrTiO_3$ and $Na_2V_6O_{16}\cdot 3H_2O$ nanowires for $BiVO_4$, see Supplementary Information Fig. SI-1) and ion-exchange to convert nanowire templates to desired materials without damaging the nanowire morphology. Fig. 2a & b show FESEM and TEM images of $Rh-SrTiO_3$ and $BiVO_4$ nanowires after ion-exchange. The nanowires have rough surfaces with mean diameters of 150 nm and 80 nm for $Rh-SrTiO_3$ and $BiVO_4$, respectively. The nanowires are phase-pure (Fig. 2c & d) with no detectable sodium after ion-exchange by energy dispersive X-ray spectroscopy (EDX). The rhodium was introduced into $SrTiO_3$ during the ion-exchange process, which shifts the light absorption onset of $SrTiO_3$ from UV to visible. The absorption onsets of $Rh-SrTiO_3$ and $BiVO_4$ nanowires were estimated to be ~700 nm and ~510 nm from the diffuse reflectance spectra as shown in Fig. 2e & f.

The $Rh-SrTiO_3$ and $BiVO_4$ nanowires exhibited stable photocatalytic activity in the production of hydrogen and oxygen from water under visible light irradiation (Supplementary Information). Hydrogen and oxygen gas evolution as a function of time during a 7-hour testing

period is shown in Fig. SI-2. The hydrogen and oxygen production rate is $\sim$ 0.26 μmol hour^{-1} based on 2 mg of Rh-SrTiO$_3$ nanowires loaded with 1 wt % Ru and $\sim$ 0.41 μmol hour^{-1} based on 2 mg of BiVO$_4$ nanowires, respectively. The measurements were carried out in a quartz container filled with 1:1 water-methanol solution for the evolution of hydrogen (methanol is used as the hole scavenger) or Fe$_2$(SO$_4$)$_3$ aqueous solution for the evolution of oxygen (Fe^{3+} is used as the electron scavenger).

After loading Ru co-catalyst on the surface of Rh-SrTiO$_3$ nanowires, the Ru/Rh-SrTiO$_3$ and BiVO$_4$ nanowires were assembled into nanowire meshes using vacuum filtration. The reason for selecting Ru as the co-catalyst instead of Pt is that Ru is an effective co-catalyst for hydrogen evolution that does not enhance back reaction for water formation from evolved H$_2$ and O$_2$.[25] Two types of nanowire mesh films were assembled including mixed Ru/Rh-SrTiO$_3$ and BiVO$_4$ nanowire mesh film and bilayer Ru/Rh-SrTiO$_3$ and BiVO$_4$ nanowire mesh film (Figure 3). Prior to photoelectrochemical testing, the nanowire mesh films were annealed at 500 – 800 $^{\circ}$C in argon to promote good contact between the Ru/Rh-SrTiO$_3$ and BiVO$_4$ nanowires.

The nanowire mesh film was tested for overall water-splitting by immersing it in deionized water with visible light irradiation ($\lambda \geq$ 400 nm). Overall water-splitting into H$_2$ and O$_2$ in a stoichiometric ratio proceeded on Ru/Rh-SrTiO$_3$ and BiVO$_4$ nanowire mesh film without using any electron mediator. Fig. 4a shows the stoichiometric evolution of H$_2$ and O$_2$ on a mixed nanowire mesh film under visible light irradiation, and there was almost no degradation of activity in three repeated runs within 18 hours. The total evolved H$_2$ and O$_2$ was $\sim$ 4.5 μmol. The turnover number of reacted electrons to the total number of Rh in Rh-SrTiO$_3$ was estimated to be $\sim$ 7.4. The photoactivity depended on the relative amount of Ru/Rh-SrTiO$_3$ to BiVO$_4$. The highest photoactivity was obtained using mixed nanowire mesh film assembled from equal amounts of Ru/Rh-SrTiO$_3$ and BiVO$_4$ nanowires. If Ru/Rh-SrTiO$_3$ nanowires alone were tested under visible light, only trace amount of H$_2$ could be produced (Fig. SI-3). On the other hand, if BiVO$_4$ nanowires were tested alone, almost no gas product was observed (Fig. SI-3), suggesting the importance of Ru/Rh-SrTiO$_3$-BiVO$_4$ interface for overall water-splitting. Since the conduction band of BiVO$_4$ is more positive than H$^+$/H$_2$ reduction potential, BiVO$_4$ itself cannot achieve overall water-splitting as photogenerated electrons in BiVO$_4$ do not have sufficient energy to reduce proton. However, when coupled with Ru/Rh-SrTiO$_3$, a two-photon z-scheme

configuration could be constructed. In this case, the minority carriers in each semiconductor participate in chemical reactions, while the majority carriers recombine at the heterojunction interface (Fig. SI-4).

The ultimate goal of applying the nanowire mesh design in solar water-splitting is to achieve simultaneous production and separation of H_2 and O_2, which is possible if a bilayer nanowire mesh is employed. Fig. 4b shows the evolution of H_2 and O_2 on a bilayer nanowire mesh film assembled from 3 mg of Ru/Rh-SrTiO$_3$ nanowires and 15 mg of BiVO$_4$ nanowires and irradiated from Ru/Rh-SrTiO$_3$ nanowire side. Stoichiometric evolution of H_2 and O_2 was evident from the beginning of the reaction. The evolution rate of H_2 and O_2 decreased if more than or less than 3 mg of Ru/Rh-SrTiO$_3$ nanowires were used while fixing BiVO$_4$ nanowires at 15 mg. This result indicated the importance of both Ru/Rh-SrTiO$_3$-BiVO$_4$ interface and the balance in light absorption by each photocatalyst in a two-photon system. The optimized evolution rate of H_2 or O_2 for a bilayer nanowire mesh was only one eighth of the optimized value for a mixed nanowire mesh. The lower photoactivity was due to the less physical contact among nanowires in a bilayer nanowire mesh film, resulting in poorer charge separation. Thus, mixing nanowires together with conductive additives such as metallic carbon nanotubes or graphene sheets during the preparation of bilayer films might lead to enhancement in the production of H_2 and O_2.[27]

In conclusion, we have demonstrated a two-photon architecture for spontaneous overall water-splitting based on the concept of nanowire meshes. These free-standing nanowire mesh networks could be made in large scales using vacuum filtration – a process used industrially to make paper, making them attractive for low cost commercial implementation. Overall water-splitting without using the electron mediators was observed for both mixed and bilayer nanowire mesh films. The bilayer film based on semiconductor nanowires can be a promising candidate for the artificial photosynthetic system.

Methods

Rh-SrTiO$_3$ and BiVO$_4$ photoelectrode preparation. This experimental procedure is described in the Supplementary Information.

Rh-SrTiO$_3$ nanowire synthesis. 6 g of anatase nanopowder (average size: 25-70 nm, Aldrich) was mixed with 50 ml of NaOH aqueous solution (15 M) at room temperature. The mixture was heated in a 125 ml Teflon-lined autoclave (Parr Instrument Co.) at 180 °C for 3 days. After the hydrothermal synthesis, the precipitates were collected and washed extensively with 0.6 M HCl aqueous solution and water to exchange Na$^+$ with H$^+$ for the

synthesis of $H_2Ti_3O_7$ nanowires. Rh-SrTiO$_3$ nanowires were synthesized from a solvothermal ion-exchange reaction using $H_2Ti_3O_7$ nanowires as the templates. Calculated amount of $H_2Ti_3O_7$ nanowires were dispersed in 40 ml of Sr(OH)$_2$ aqueous-ethanol solution ($V_{ethanol}$: V_{water} = 4 : 1). The molar ratio of strontium to titanium was fixed at 1.5. Following, 1 mole % (Rh/Ti = 1/99) of Rh(NO$_3$)$_3$ was added into the suspension and the mixture was autoclaved in a 45 ml Teflon-lined autoclave (Parr Instrument Co.) at 120 °C for 2 days. After completion of the reaction, the harvested precipitates were washed repeatedly with 0.1 M formic acid to remove residue SrCO$_3$ and water, and dried in ambient air. The final products were calcined at 800 °C for 4 hours.

BiVO$_4$ nanowire synthesis. 1 mmol of V_2O_5 power and 2 mmol of Na$_2$SO$_4$ were mixed in 30 ml of deionized water at room temperature. The mixture was heated in a 45 ml Teflon-lined autoclave at 180 °C for 24 hours for the synthesis of Na$_2$V$_6$O$_{16}$·3H$_2$O nanowire templates.[28] Following, calculated amount of Na$_2$V$_6$O$_{16}$·3H$_2$O nanowires were mixed with Bi(NO$_3$)$_3$·5H$_2$O (Bi/V = 1) in 40 ml of ethanol-water solution ($V_{ethanol}$: V_{water} = 4 : 1). The mixture was autoclaved in a 45 ml Teflon-lined autoclave at 120 °C for 24 hours to convert Na$_2$V$_6$O$_{16}$·3H$_2$O nanowires into monoclinic BiVO$_4$ nanowires.

Nanowire characterization. The crystal structure of the as-synthesized nanowires was examined by X-ray diffraction (XRD, Bruker D8 X-ray diffractometer D71). Morphological and lattice structural information were examined with field emission scanning electron microscopy (FESEM, JSM-6340F), transmission electron microscopy, selected area electron diffraction, and energy dispersive X-ray spectroscopy (TEM/SAED/EDX, Hitachi H-7650). The optical absorption spectra were recorded using a UV-vis-NIR scanning spectrophotometer equipped with an integration sphere (Shimadzu UV-3101PC).

Co-catalyst loading. Ru co-catalysts (1 wt %) working as active sites for hydrogen evolution were loaded on Rh-SrTiO$_3$ nanowires by photodeposition from an aqueous-methanol solution (10 vol % methanol) containing calculated amount of RuCl$_3$·nH$_2$O. The Ru-loaded Rh-SrTiO$_3$ nanowires were harvested by filtration and washed with deionized water and dried in ambient air.

Nanowire mesh fabrication. The nanowire mesh networks were assembled by filtration of a nanowire suspension onto a filter membrane. For example, to fabricate bilayer Ru/Rh-SrTiO$_3$ and BiVO$_4$ nanowire mesh films, Ru/Rh-SrTiO$_3$ and BiVO$_4$ nanowires were first suspended in deionized water in two separate containers. The BiVO$_4$ nanowire suspension was filtered on a vacuum-filtration setup using PVDF filter membrane (Durapore, 0.5 μm pore size), followed by filtering the Ru/Rh-SrTiO$_3$ nanowire suspension. After filtration, the films on the filter membrane were allowed to dry in ambient air. Once completely dried, the nanowire mesh films could be detached from the filter membrane as free standing discs. To promote good physical contact between Ru/Rh-SrTiO$_3$ and BiVO$_4$ nanowires, the nanowire mesh films were annealed at 500 – 800 °C in argon.

Photoelectrochemical experiment. Photocurrent of linked photoelectrochemical cell system was measured in a two-electrode cell without applying any external bias in a sealed Teflon reactor with a quartz window on its side wall for illumination. A 1M NaOH aqueous solution was used as the electrolyte. The illumination was from a 300 W Xe lamp which passes through a long-pass filter with cutoff at 400 nm. During photochemical reactions, photocurrent and amounts of gas products were measured using a potentiostat (Electrochemical Workstation Zive SP2) and an inline gas chromatography (Agilent 490 MicroGC). The photocatalytic activity of the nanowire mesh

films was evaluated using inline gas chromatography (Agilent 3000 MicroGC, MS-5A column, TCD, Ar carrier). The nanowire mesh film was suspended in pH = 3.5 deionized water (adjusted using dilute H_2SO_4) inside a side-window cell made of quartz, which is connected to a gas-closed circulation system. The solution was evacuated to remove dissolved air and purged with Ar before irradiation. The light source was a 450 W Xe lamp with a long-pass filter ($\lambda \geq 400$ nm) sitting in between the light source and the quartz reactor. The amounts of evolved gases were periodically determined with an inline gas chromatography.

Author contributions

B.L., C.H.W., and P.Y. designed and conceived the research. B.L., J.W.M. and H.Y.W. prepared the materials. B.L., J.W.M. and C.H.W. performed the experiments. B.L., C.H.W., and P.Y. analyzed the data. B.L. and P.Y. wrote the manuscript.

Additional information

The authors declare no competing financial interests. Supplementary information accompanies this paper at... Reprints and permission information is available online at... Correspondence and requests for materials should be addressed to P.Y.

Reference

1   Bard, A. J. & Fox, M. A. Artificial photosynthesis - solar splitting of water to hydrogen and oxygen. *Accounts Chem. Res.* **28**, 141-145 (1995).

2   Fujishima, A., Zhang, X. T. & Tryk, D. A. TiO_2 photocatalysis and related surface phenomena. *Surf. Sci. Rep.* **63**, 515-582 (2008).

3   Kudo, A. & Miseki, Y. Heterogeneous photocatalyst materials for water splitting. *Chem. Soc. Rev.* **38**, 253-278 (2009).

4   Khan, S. U. M., Al-Shahry, M. & Ingler, W. B. Efficient photochemical water splitting by a chemically modified n-TiO_2. *Science* **297**, 2243-2245 (2002).

5   Zou, Z. G., Ye, J. H., Sayama, K. & Arakawa, H. Direct splitting of water under visible light irradiation with an oxide semiconductor photocatalyst. *Nature* **414**, 625-627 (2001).

6   Kato, H., Asakura, K. & Kudo, A. Highly efficient water splitting into H_2 and O_2 over lanthanum-doped $NaTaO_3$ photocatalysts with high crystallinity and surface nanostructure. *J. Am. Chem. Soc.* **125**, 3082-3089 (2003).

7   Maeda, K. *et al.* Photocatalyst releasing hydrogen from water - Enhancing catalytic performance holds promise for hydrogen production by water splitting in sunlight. *Nature* **440**, 295-295 (2006).

8   Kato, H., Hori, M., Konta, R., Shimodaira, Y. & Kudo, A. Construction of Z-scheme type heterogeneous photocatalysis systems for water splitting into H_2 and O_2 under visible light irradiation. *Chem. Lett.* **33**, 1348-1349 (2004).

9   Abe, R., Sayama, K. & Sugihara, H. Development of new photocatalytic water splitting into H_2 and O_2 using two different semiconductor photocatalysts and a shuttle redox mediator IO^{3-}/I^-. *J. Phys. Chem. B* **109**, 16052-16061 (2005).

10   Maeda, K., Higashi, M., Lu, D. L., Abe, R. & Domen, K. Efficient nonsacrificial water splitting through two-step photoexcitation by visible light using a modified oxynitride as a hydrogen evolution photocatalyst. *J. Am. Chem. Soc.* **132**, 5858-5868 (2010).

11   Fujishima, A. & Honda, K. Electrochemical photolysis of water at a semiconductor electrode. *Nature* **238**, 37-38 (1972).

12   Ohashi, K., McCann, J. & Bockris, J. O. M. Stable photoelectrochemical cells for splitting of water. *Nature* **266**, 610-611 (1977).

13   Sun, J. W., Liu, C. & Yang, P. D. Surfactant-free, large-scale, solution-liquid-solid growth of gallium phosphide nanowires and their use for visible-light-driven hydrogen production from water reduction. *J. Am. Chem. Soc.* **133**, 19306-19309 (2011).

14   Cesar, I., Kay, A., Martinez, J. A. G. & Gratzel, M. Translucent thin film Fe_2O_3 photoanodes for efficient water splitting by sunlight: Nanostructure-directing effect of Si-doping. *J. Am. Chem. Soc.* **128**, 4582-4583 (2006).

15   Gao, H. W., Liu, C., Jeong, H. E. & Yang, P. D. Plasmon-enhanced photocatalytic activity of iron oxide on gold nanopillars. *Acs Nano* **6**, 234-240 (2012).

16   Santato, C., Odziemkowski, M., Ulmann, M. & Augustynski, J. Crystallographically oriented mesoporous WO_3 films: Synthesis, characterization, and applications. *J. Am. Chem. Soc.* **123**, 10639-10649 (2001).

17   Kudo, A., Omori, K. & Kato, H. A novel aqueous process for preparation of crystal form-controlled and highly crystalline $BiVO_4$ powder from layered vanadates at room temperature and its photocatalytic and photophysical properties. *J. Am. Chem. Soc.* **121**, 11459-11467 (1999).

18   Jia, Q., Iwashina, K. & Kudo, A. Facile fabrication of an efficient $BiVO_4$ thin film electrode for water splitting under visible light irradiation. *Proc. Natl. Acad. Sci. USA* **109**, 11564-11569 (2012).

19   Abe, R., Higashi, M. & Domen, K. Facile Fabrication of an efficient oxynitride TaON photoanode for overall water splitting into H_2 and O_2 under visible light irradiation. *J. Am. Chem. Soc.* 132, 11828-11829 (2010).

20   Higashi, M., Domen, K. & Abe, R. Fabrication of efficient TaON and Ta_3N_5 photoanodes for water splitting under visible light irradiation. *Energy Environ. Sci.* **4**, 4138-4147 (2011).

21   Konta, R., Ishii, T., Kato, H. & Kudo, A. Photocatalytic activities of noble metal ion doped $SrTiO_3$ under visible light irradiation. *J. Phys. Chem. B* **108**, 8992-8995 (2004).

22   Iwashina, K. & Kudo, A. Rh-Doped $SrTiO_3$ Photocatalyst electrode showing cathodic photocurrent for water splitting under visible-light rrradiation. *J. Am. Chem. Soc.* **133**, 13272-13275 (2011).

23   Zhang, F. X. *et al.* Cobalt-modified porous single-crystalline $LaTiO_2N$ for highly efficient water oxidation under visible light. *J. Am. Chem. Soc.* **134**, 8348-8351 (2012).

24   Nozik, A. J. Photochemical diodes. *Appl. Phys. Lett.* **30**, 567-569 (1977).

25   Sasaki, Y., Nemoto, H., Saito, K. & Kudo, A. Solar water splitting using powdered photocatalysts driven by Z-schematic interparticle electron transfer without an electron mediator. *J. Phys. Chem. C* **113**, 17536-17542 (2009).

26   Yang, P. D. & Tarascon, J. M. Towards systems materials engineering. *Nat. Mater.* **11**, 560-563 (2012).

27   Iwase, A., Ng, Y. H., Ishiguro, Y., Kudo, A. & Amal, R. Reduced graphene oxide as a solid-state electron mediator in Z-scheme photocatalytic water splitting under visible light. *J. Am. Chem. Soc.* **133**, 11054-11057 (2011).

28   Zhou, G. T., Wang, X. C. & Yu, J. C. Selected-control synthesis of NaV_6O_{15} and $Na_2V_6O_{16} \cdot 3H_2O$ single-crystalline nanowires. *Cryst. Growth Des.* **5**, 969-974 (2005).
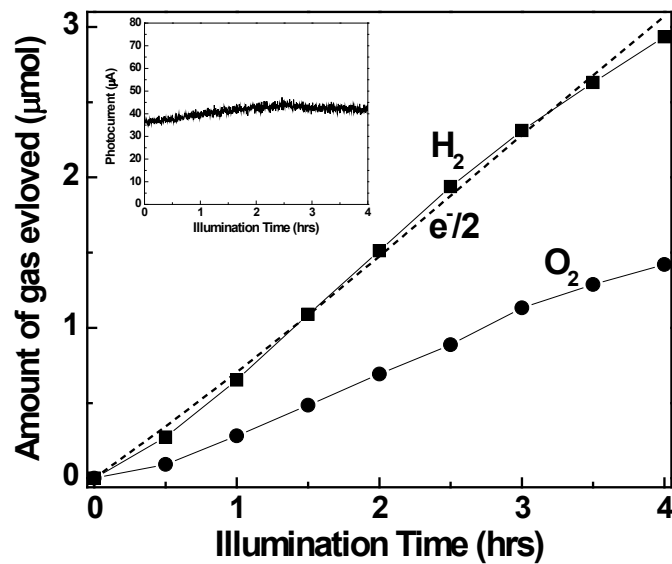
Figure 1 | Self-driving photoelectrochemical cells made from Rh-SrTiO₃ photocathode and BiVO₄ photoanode. Photoelectrochemical overall water splitting over linked Rh-SrTiO₃ and BiVO₄ photoelectrodes without applying any external bias under visible light irradiation. Dashed line: half amount of electrons which had passed through the external circuit of linked photoelectrochemical cell.
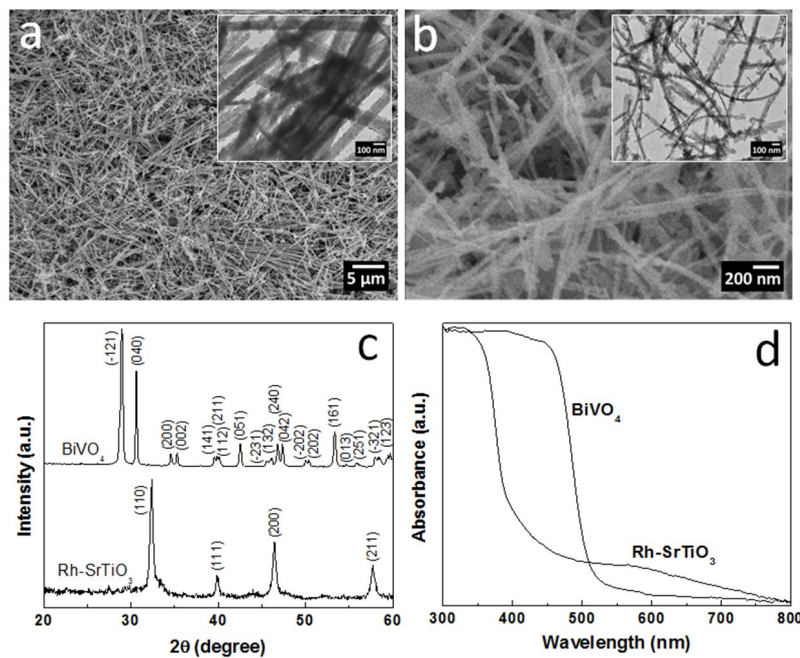
Figure 2 | Rh-SrTiO₃ and BiVO₄ nanowires. a and **b**, FESEM and TEM images of Rh-SrTiO₃ and BiVO₄ nanowires, respectively. **c,** XRD patterns of Rh-SrTiO₃ and BiVO₄ nanowires. **d,** UV-vis absorption spectra of Rh-SrTiO₃ and BiVO₄ nanowires showing the absorption onsets.
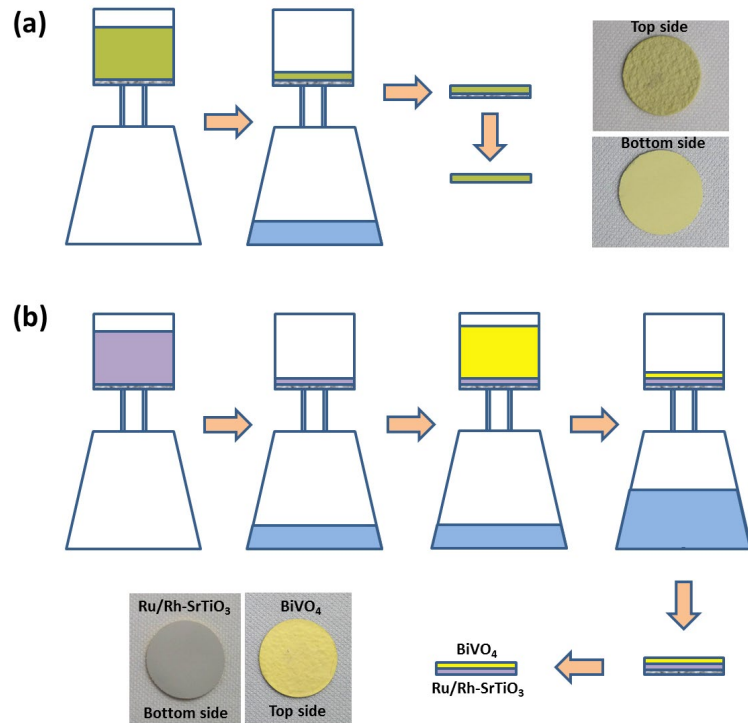
Figure 3 | Formation of mixed and bilayer Ru/Rh-SrTiO₃ and BiVO₄ nanowire mesh. a and **b**, Schematic illustrations of formation of mixed and bilayer Ru/Rh-SrTiO₃ and BiVO₄ nanowire mesh films.
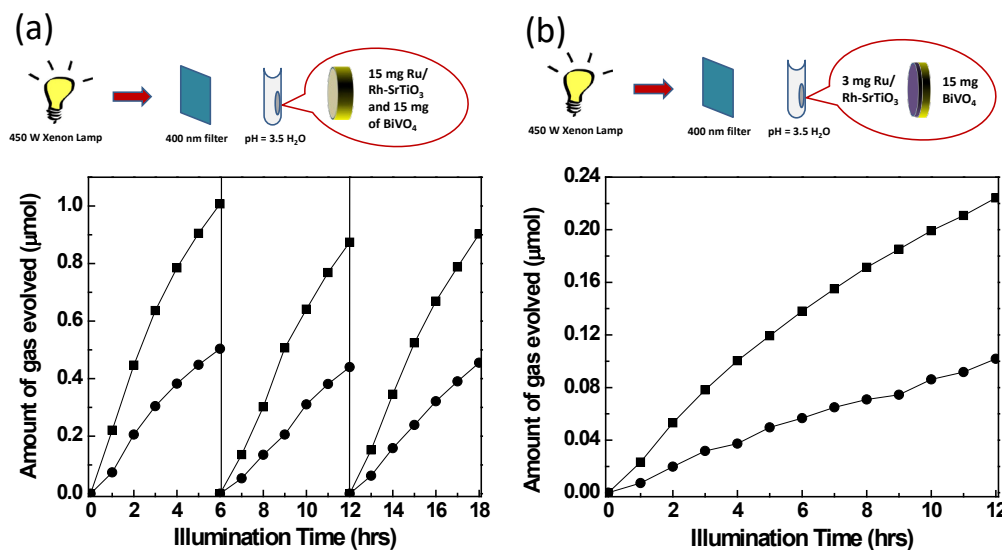
Figure 4 | Overall water-splitting under visible light irradiation. a, Cycling measurements of hydrogen (■) and oxygen (●) evolution from overall photocatalytic water splitting using mixed Ru/Rh-SrTiO$_3$ and BiVO$_4$ nanowire mesh film. **b,** Overall water splitting into hydrogen (■) and oxygen (●) using bilayer Ru/Rh-SrTiO$_3$ and BiVO$_4$ nanowire mesh film.